JOURNAL OF GENERAL VIROLOGY

RESEARCH ARTICLE

Mahmoud *et al.*, *Journal of General Virology* 2024;105:001949

DOI 10.1099/jgv.0.001949

MICROBIOLOGY SOCIETY

OPEN ACCESS

# Cyclooxygenase-2/prostaglandin E2 pathway regulates infectious bronchitis virus replication in avian macrophages

Motamed Elsayed Mahmoud[1,2], Muhammad Farooq[1], Ishara M. Isham[1], Ahmed Ali[1,3], Mohamed S.H. Hassan[1,4], Heshanthi Herath-Mudiyanselage[1], Hiruni A. Ranaweera[1], Shahnas M. Najimudeen[1] and Mohammad Faizal Abdul-Careem[1,*]

**Abstract**

Infectious bronchitis virus (IBV) is a significant respiratory pathogen that affects chickens worldwide. As an avian coronavirus, IBV leads to productive infection in chicken macrophages. However, the effects of IBV infection in macrophages on cyclooxygenase-2 (COX-2) expression are still to be elucidated. Therefore, we investigated the role of IBV infection on the production of COX-2, an enzyme involved in the synthesis of prostaglandin E2 (PGE2) in chicken macrophages. The chicken macrophage cells were infected with two IBV strains, and the cells and culture supernatants were harvested at predetermined time points to measure intracellular and extracellular IBV infection. IBV infection was quantified as has been the COX-2 and PGE2 productions. We found that IBV infection enhances COX-2 production at both mRNA and protein levels in chicken macrophages. When a selective COX-2 antagonist was used to reduce the COX-2 expression in macrophages, we observed that IBV replication decreased. When IBV-infected macrophages were treated with PGE2 receptor (EP2 and EP4) inhibitors, IBV replication was reduced. Upon utilizing a selective COX-2 antagonist to diminish PGE2 expression in macrophages, a discernible decrease in IBV replication was observed. Treatment of IBV-infected macrophages with a PGE2 receptor (EP2) inhibitor resulted in a reduction in IBV replication, whereas the introduction of exogenous PGE2 heightened viral replication. Additionally, pretreatment with a Janus-kinase two antagonist attenuated the inhibitory effect of recombinant chicken interferon (IFN)-γ on viral replication. The evaluation of immune mediators, such as inducible nitric oxide (NO) synthase (iNOS), NO, and interleukin (IL)–6, revealed enhanced expression following IBV infection of macrophages. In response to the inhibition of COX-2 and PGE2 receptors, we observed a reduction in the expressions of iNOS and IL-6 in macrophages, correlating with reduced IBV infection. Overall, IBV infection increased COX-2 and PGE2 production in addition to iNOS, NO, and IL-6 expression in chicken macrophages in a time-dependent manner. Inhibition of the COX-2/PGE2 pathway may lead to increased macrophage defence mechanisms against IBV infection, resulting in a reduction in viral replication and iNOS and IL-6 expressions. Understanding the molecular mechanisms underlying these processes may shed light on potential antiviral targets for controlling IBV infection.

## INTRODUCTION

Infectious bronchitis virus (IBV) is an avian virus belonging to the Coronaviridae family. IBV primarily affects the chicken respiratory tract, resulting in respiratory distress, reduced production, and increased susceptibility to secondary bacterial infections [1, 2]. Like the challenges posed by severe acute respiratory syndrome coronavirus 2 (SARS-CoV-2) [3], the IBV exhibits a diverse range of serotypes and genotypes, contributing to the reduced reliability of vaccination-based control strategies [3–7]. Although IBV targets epithelial cells in the respiratory, urogenital, gastrointestinal, and reproductive tracts

Received 05 October 2023; Accepted 19 December 2023; Published 08 January 2024

**Author affiliations:** [1]Faculty of Veterinary Medicine, University of Calgary, 3330 Hospital Drive NW, Calgary, AB, T2N 4N1, Canada; [2]Department of Animal Husbandry, Faculty of Veterinary Medicine, Sohag University, Sohag 84524, Egypt; [3]Department of Pathology, Faculty of Veterinary Medicine, Beni-Suef University, Beni Suef, 62521, Egypt; [4]Department of Avian and Rabbit Medicine, Faculty of Veterinary Medicine, Assiut University, Assiut 71515, Egypt.
***Correspondence:** Mohammad Faizal Abdul-Careem, faizal.abdulcareem@ucalgary.ca

**Keywords:** infectious bronchitis virus; chicken macrophage; cyclooxygenase-2 inhibitor; prostaglandin receptor antagonist; janus-kinase inhibitor.

**Abbreviations:** Conn, Connecticut; COX, cyclooxygenase; DMV, Delmarva; EP, prostaglandin E2 receptor; HIV, human immunodeficiency virus; IAV, influenza A virus; IBV, infectious bronchitis virus; IFN-γ, interferon gamma; IL-6, interleukin-6; iNOS, inducible nitric oxide synthase; JAK, Janus Kinase; LPS, lipopolysaccharide; MDV, Marek's disease virus; MOI, multiplicity of infection; NF-κB, nuclear factor-kappa B; NO, Nitric oxide; $NO_2$, nitrite; PGE2, prostaglandin E2; SARS-CoV-2, severe acute respiratory syndrome coronavirus 2; TLR, toll-like receptor.

Three supplementary figures and one supplementary material are available with the online version of this article.

[8], it has been shown that lymphoid cells such as monocytes [9] and macrophages [10] are also infected, leading to productive infections, which are vital for viral pathogen recognition and clearance [11]. These phagocytic cells not only engulf and present viral antigens and clear virus particles but also release antiviral mediators and various effector molecules that regulate the immune response [12–15].

Cyclooxygenases (COXs) catalyse the rate-limiting step in the production of prostaglandins (PGs) [16]. The COX-1 is the constitutively expressed isoenzyme in the plasma membrane of the cells, whereas COX-2 is the inducible form expressed in the membrane of endoplasmic reticulum [16, 17]. The enzyme COX-2 is involved in the production of PGs and their downstream product prostaglandin E2 (PGE2) in particular, which appears to play various roles in cellular processes, including inflammation [18, 19]. COX-2 purification and cloning has opened the gate for a possible synthesis of selective blockers that reduce inflammation without removing the protective PGs in the stomach and kidney made by COX-1 [20]. COX-2 expression and subsequent PGE2 production in macrophages are regulated in response to various inflammatory and viral agents [21, 22].

PGE2 has been recognized for its immunosuppressive properties [21, 23]. PGE2 receptors play crucial roles in mediating various physiological processes in birds [24]. Mammals possess several types of PGE2 receptors, which are classified into four main subtypes: EP1, EP2, EP3, and EP4. Among these subtypes, EP2, EP3 and EP4, are proposed to play crucial roles under both physiological and pathological conditions in chickens, whereas EP1 is highly likely to be lost in the avian lineage [25, 26].

The role of COX-2 in avian herpesvirus infections, such as Marek's disease virus (MDV) infection, has been demonstrated [27, 28]. These studies indicate that MDV activates the COX-2/PGE2 pathway both in chickens and *in vitro* using a chicken embryonic fibroblasts model, leading to immunosuppression characterized by a reduction in T-cell proliferation. Consequently, this results in an increase in viral replication, actions attributed to the activation of the PGE2 receptors 2 (EP2) and 4 (EP4) signalling pathways.

In an *in vivo* study involving the IBV DMV/1639 strain, it was shown that IBV replicates in both the primary and secondary immune organs of newly hatched chicks, resulting in significant structural alterations correlating with augmented COX-2 mRNA expression in the spleen and thymus [29]. Moreover, in mature chickens, IBV inoculation resulted in elevated mRNA expression of COX-2 and heightened levels of PGE2 in the uterine mucosa [30].

Much like mammals, birds harbour diverse viral-sensing pattern recognition receptors (PRRs), notably toll-like receptors (TLRs). Avian TLR3 and TLR7 are central to RNA virus recognition [31]. Infection with IBV, as a single stranded RNA virus, may trigger the activation of the TLR7 signalling pathway in the target tissue [32, 33], like many viruses leading to the activation of the nuclear transcription factor NF-κB and ultimately resulting in the induction of proinflammatory cytokine production [34]. Inducible nitric oxide synthase (iNOS) and interleukin (IL)-6 are also pivotal components of the chicken's immune response against IBV infection [35, 36]. The enzyme iNOS catalyses the production of nitric oxide (NO), which is known for its antiviral defence role [37]. Upregulation of iNOS expression in response to viral infections, including IBV, leads to increased NO levels via inhibiting viral proteases suppressing its replication and spread [38, 39]. Elevated IL-6 levels in IBV-infected chickens further underscore its role in orchestrating the immune response, activating essential downstream immune pathways involving B and T cells for effective antiviral defence [36, 37]. IL-6 serves as a signalling molecule that triggers various downstream immune responses, including the activation of B and T cells, which are essential for mounting an effective antiviral response [40].

IBV targets macrophages, leading to modulation of macrophage responses [10, 41]. However, the influence of IBV replication in the COX-2/PGE2 pathway is unknown. Hence, investigating the role of molecules involved in the COX-2/PGE2 pathway in IBV-infected macrophages is crucial for unravelling the interplay between the IBV and avian macrophages. The objective of the study was to determine if IBV is capable of inducing molecules involved in the COX-2/PGE2 pathway and to investigate the impact of these molecules on IBV replication in avian macrophages.

## METHODS

### The virus

Two strains of IBV, Canadian IBV DMV/1639 (DMV/1639) and Connecticut (Conn A5968) were used. The molecular characterization and titration of the IBV DMV1639 strain has been described previously in detail [42, 43]. The IBV Conn A5968 strain was purchased from the American Type Culture Collection (ATCC, Manassas, Virginia, USA) and used in previous studies [10, 32].

### Chicken macrophage cells

The chicken macrophage cell line MQ-NCSU [44] was kindly provided by Dr Shayan Sharif (University of Guelph, ON, Canada). As previously described [10], the macrophage cell line was grown in an LM-Hahn medium, supplemented with 8% fetal bovine serum (FBS), 10% chicken serum, 1% antibiotic/antimycotic, and 10 µM 2-Mercaptoethanol. All cell culture reagents were purchased from Gibco Life Technologies Corporation (Gibco Life Technologies, Burlington, ON, Canada).

### Reagents

The subsequent pharmaceuticals, including the selective COX-2 inhibitor SC-236, PGE2, Janus Kinase (JAK)-I inhibitor 420099, and JAK-II inhibitor SP600125, were procured from Millipore Sigma (Sigma Aldrich, Burlington, Massachusetts, USA). All compounds were dissolved in dimethyl sulfoxide (DMSO; Thermo Fisher Scientific, Rockford, Illinois, USA).

### Experimental design

The MQ-NCSU cells were seeded in 12-well plates at $1.5\times10^6$ ml$^{-1}$ complete media and incubated at 40°C for 24 hours (h) in a humidified incubator (5% $CO_2$). After 24 h, the LM-Hahn complete media was replaced with serum-free media and IBV was inoculated at 0.1 multiplicity of infection (MOI), including mock infected controls that received Dulbecco's phosphate-buffered saline (dPBS, Sigma Aldrich, Burlington, Massachusetts, USA). At 3, 6, 12, 24 and 48 h post-infection (hpi), the culture supernatants were collected, and the cells were washed three times with dPBS before being homogenized in Trizol reagent (Invitrogen Canada Inc., Burlington, ON, Canada). The homogenates and culture supernatants were frozen at −80°C for further analyses.

### RNA extraction and reverse transcription

Total cellular and culture supernatant RNA were extracted using Trizol reagent according to the manufacturer's protocol (Invitrogen Canada Inc., Burlington, ON, Canada). Purified RNA was quantified by the Nanodrop 1000 spectrophotometer (Thermo Scientific, Wilmington, DE, USA). A complementary (c)DNA was synthesised from 2 µg of cellular RNA and 1 µg of culture supernatant fluid RNA using the SuperScript IV Reverse Transcriptase kit (Thermo Fisher Scientific, Rockford, Illinois, USA).

### Determination of IBV genome load and immune gene mRNA expression

Real-time quantitative polymerase chain reaction (qPCR) (CFX Opus Realtime PCR systems, BioRAD, USA) assay was used for amplifying the IBV genome load and immune gene mRNA expressions in 96-well plates (VWR, AB, Canada). All samples were run in duplicate following the reaction protocol: 95°C for 20 seconds (s), 39 cycles of extension/amplification 95°C for 3 s, and 60°C for 30 s, and then annealing at 95°C for 10 s. The primer sequences used were published previously [29]. SYBR green qPCR assay format was used and included three segment melt-curve analyses at 95°C for 3 s, 65°C for 5 s, 9°C for 5 s, respectively. Based on a linear dynamic range of 1–7 log10 copies/reaction, we calculated the number of viral genome copies. The relative mRNA expressions of COX-2, iNOS, IL-1β, and IL-6 were calculated based on normalized individual values for the housekeeping gene β-actin.

### Indirect immunofluorescence assay

Double immunofluorescence staining for colocalization of IBV-antigen and COX-2 protein was carried out in macrophages as previously described [45, 46]. The cells were grown on glass coverslips (VWR International, Radnor, Pennsylvania, USA) in 12-well plates (Corning Incorporated, Corning, New York, USA). The cells were washed twice with dPBS to remove non-adherent cells and then fixed with 3.6% paraformaldehyde (Sigma Aldrich, Burlington, Massachusetts, USA) at the indicated time points. The MQ-NCSU cell wall was stained with 10 µg ml$^{-1}$ wheat germ agglutinin conjugated to Alexa fluor 350 (Sigma Aldrich, Burlington, Massachusetts, USA) for 30 minutes (min) at room temperature in darkness. Then, the cells were washed with Hanks' Balanced Salt Solution (HBSS, Gibco, Thermo Fisher Scientific, Grand Island, New York, USA) to remove the stain. The cells were permeabilized by adding 200 µl of 0.2% Triton-X100 (Sigma Aldrich, Burlington, Massachusetts, USA) (in HBSS) per well. Non-specific bindings were blocked by 1 h incubation with 1 ml per well of 2.5% horse serum at room temperature. Then, the cells were incubated with the primary monoclonal antibodies against the IBV-N antigen (Novus Biologicals, Centennial, Colorado, USA), and COX-2 (Cell Signalling Technology, Danvers, Massachusetts, USA) at a dilution of 1:400 in 2.5% horse serum was applied for 1 h at room temperature. The cells were washed twice in Tris-buffered saline solution (TBSS) and once in HBSS. The cells were incubated with the VectaFluor Excel Amplified Kit, anti-Mouse IgG, DyLight 594 for the IBV antigen and with the VectaFluor Horse Anti-Rabbit IgG, DyLight 488 Antibody Kit for the COX-2 protein, respectively (Vector Laboratories, Burlingame, California, USA). The incubation was for 15 min with the antibodies and 20 min with the amplifiers. Finally, the coverslips were fixed by VECTASHIELD Vibrance antifade mounting medium with 4′,6-diamidino-2-phenylindole (DAPI, Vector Laboratories, Burlingame, California, USA). Subsequently, the cells were subjected to incubation with the VectaFluor Excel Amplified Kit, anti-Mouse IgG, DyLight 594 targeting the IBV antigen and with the VectaFluor Horse Anti-Rabbit IgG, DyLight 488 Antibody Kit targeting the COX-2 protein, respectively. The incubation period lasted 15 min for the antibodies and 20 min for the amplifiers. Lastly, coverslips were affixed using VECTASHIELD Vibrance antifade mounting medium containing DAPI for nuclear staining (Vector Laboratories, Burlingame, California, USA). They were then stored in a dark environment at 4°C for imaging purposes. Visualization of cells was performed by Nikon Spectral Confocal Microscopy System (Nikon Corporation, Tokyo, Japan).

Five different microscopic fields with the highest fluorescent signals for IBV-N antigens and COX-2 proteins were captured per replicate together with the relevant nuclear stained (DAPI) areas. The area percentage of fluorescent signals was calculated using Image-J software (National Institute of Health, Bethesda, Maryland, USA), as previously described [10].

### Western blot

MQ-NSCU cells were seeded in a six-well plate at $1.5\times10^6$ ml$^{-1}$ and kept for 24 h until they reached >90% confluence, as previously described [44]. The cells were scraped after adding 300 µl of a cocktail of cell lytic buffer (cellytic mt cell lysis reagent: Sigma-Aldrich, St. Louis, Missouri, USA) and protease inhibitor (Millipore Sigma, Sigma Aldrich, Burlington, Massachusetts, USA). The cell lysate was incubated at 37°C on a shaking platform for 15 min, and then spun down at 12000 ***g*** for 15 min. Protein content was measured using the Pierce Rapid Gold BCA protein assay kit (Thermo Scientific, Rockford, Illinois, USA). Laemllii buffer (5 x, Bio-Rad Laboratories, Hercules, California, USA) was added, and the mixture was denatured by heating at 95°C for 10 min. Aliquots of samples containing 20 µg of protein were loaded onto 10 % acrylamide gel (Bio-Rad Laboratories, Hercules, California, USA). They were electrophoresed at 80 V for 20 min followed by 200 V for 60 min. The protein was transferred to a methanol-activated PVDF membrane (0.45 µm) (Merck Millipore Corporation Inc., Darmstadt, Germany) in a semi-dry chamber (Bio-Rad Laboratories, Hercules, California, USA). The electrical transfer was set up at 2.5 A and 25 V for 45 min. The membrane was blocked by incubation in 4% goat serum at RT for 1 h on a rocking platform. It was then incubated for 1 h on a rocking platform with 1:25000 goat anti-mouse β-actin (Sigma-Aldrich Corporation, St. Louis, Missouri, USA) and 1:1000 goat anti-rabbit COX-2 monoclonal antibodies (Sigma-Aldrich Corporation, St. Louis, Missouri, USA). After five washes with TBSS, the secondary antibodies were applied for 1 h with shaking, and then the blot was exposed to a further five washes. The ChemiDoc Imaging System (Bio-Rad Laboratories, Inc., Hercules, California, USA) was used to visualize the plot after 5 min immersion in the chemiluminescence dye (Immobilon R Forte Western HRP substrate: Merck Millipore Corporation, Burlington, Massachusetts, USA).

### Extracellular PGE2 ELISA

Prostaglandin E2 (PGE2) levels in the culture supernatant of MQ-NCSU cells were measured using the PGE2 assay kit (R and D Systems, Minneapolis, Minnesota, USA). The PGE2 assay was performed according to the manufacturer's guidelines. This included blank wells, standards, and positive and negative controls. The absorbance was read at 450 nm in the horizontal microplate reader (680 XR, Microplate Reader, Bio-Rad, Hercules, California, USA), and PGE2 concentrations in the culture supernatant were calculated based on the generated standard curve.

### Intracellular COX-2 assay

Cell lysates were prepared according to the instructions in the COX-2 Simple-Step ELISA Kit (Abcam, Cambridge, Massachusetts, USA). Samples were run in duplicate and the data were plotted against the linear standard curve of the recombinant COX-2 protein provided in the kit.

### Nitric oxide (NO) production

The NO production was measured in the culture supernatants using a nitrate/nitrite colorimetric assay kit (Cayman Chemical Company, Ann Arbor, Michigan, USA). Nitrite ($NO_2$) net amounts were obtained from the sum of both nitrite and nitrate after subtracting them from a cell-free medium, according to the manufacturer's recommendations. All samples were run in duplicate, and the $NO_2$ was calculated based on linear standard $NO_2$ curve absorbance at 595 nm in a plate reader (680 XR, Microplate Reader, Bio-Rad, Hercules, California, USA).

### Statistical analysis

GraphPad Prism software (version 9.5.1; 733, GraphPad Software, San Diego, California, USA) was used to perform the statistical analysis. Two-way ANOVA was selected for the two IBV strains or treatments×multiple time-points experiments, and one-way ANOVA was selected for the two strains or multiple treatments×one time-point experiments. ANOVA was followed by Bonferroni's post-hoc test for multiple comparisons. The differences between means were considered significant if $P<0.05$%.

## RESULTS

### IBV replication in chicken macrophages

The time-dependent expression patterns of the viral genome load for IBV DMV/1639 and IBV Conn A5968 strains are illustrated in Fig. 1a, b. The intracellular IBV Conn A5968 strain viral genome load was significantly higher than the IBV DMV/1639 genome load at 3, 6, and 12 hpi (Fig. 1a: $P<0.0001$, and $P<0.0001$) and at 12 and 48 hpi in the culture supernatants (Fig. 1b: $P<0.0001$ and $P<0.0001$). While the detection of the IBV-N antigen showed relatively low signalling at three hpi compared to other time points, as detailed in Figs 1d and S1 a–j, available in the online version of this article the percentage of IBV-N protein staining for the IBV Conn A5968 strain was significantly higher than that of the DMV/1639 strain at both 6 and 48 hpi (Fig. 1b, c: $P<0.0001$ and $P<0.0001$, respectively). The immunofluorescence images depict the IBV-N antigen localization inside the IBV-infected MQ-NCSU cells at 3, 6, 12, 24, and 48 hpi compared to the isotype control (Fig. 1d). These data indicate that the N-antigen of two strains of IBV – DMV/1639 and Conn A5968 – had a different expression pattern in chicken macrophages.

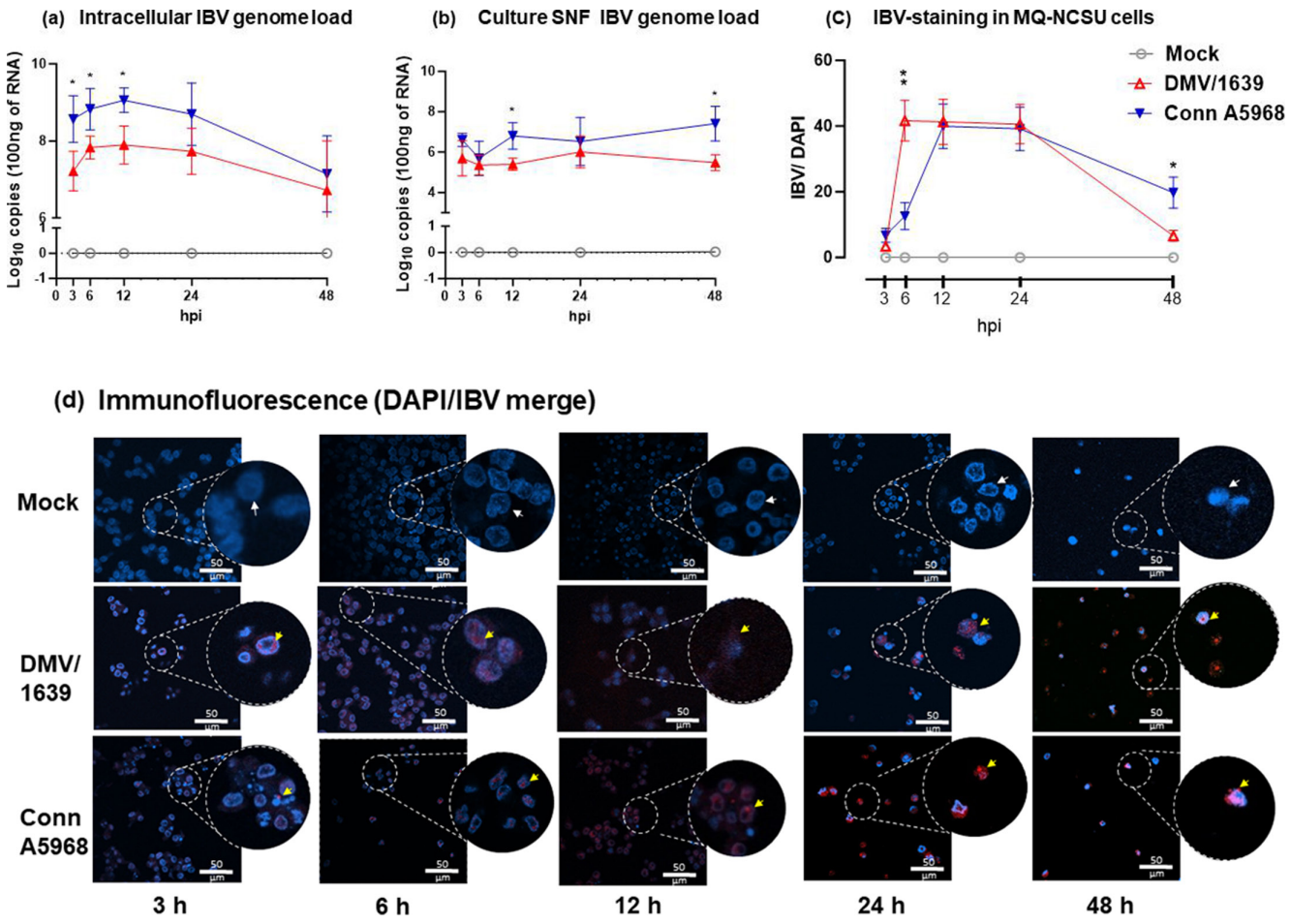


**Fig. 1.** Replication of IBV in avian macrophages. MQ-NCSU cells were seeded at $1.5\times10^6$ cells $ml^{-1}$ in 12-well culture plates and infected with IBV DMV/1639 or IBV Conn A5968 at an MOI of 0.1 maintaining uninfected controls. The IBV genome load was quantified in cells (a) and culture supernatants (b) at 3, 6, 12, 24, and 48 hpi following RNA extraction and cDNA synthesis. (c) The graph in panel C shows the mean fluorescence intensities of IBV-N protein expression. The data presented herein represents the mean±SD of two independent experiments, each conducted in triplicate. Statistical analysis using Bonferroni post-hoc testing following a two-way ANOVA revealed significant differences among means with distinct superscripts. Statistical significance was established at a threshold of $P<0.05$. (d) Representative confocal microscopy images depict the intracellular viral protein. For c and d, macrophages were cultured on glass coverslips in 12-well plates before being infected with IBV. At the indicated time points, the cell membranes were stained with wheat germ agglutinin (10 µg $ml^{-1}$) conjugated to Alexa fluor 350 (blue in colour) for 30 min before being fixed with 4% cold paraformaldehyde and stained for IBV-N antigen (Dylight 594). Nuclei were stained with DAPI included in the anti-fade mounting medium. The white arrows point to the cells, and the yellow arrows point to IBV-N protein. Data represent mean±SD of two independent experiments done in triplicate. The means with different superscripts were significantly different. Statistical significance was considered when $P<0.05$.

## The IBV infection in chicken macrophages leads to COX-2 production

To investigate whether COX-2 was induced in chicken macrophages infected with IBV, we determined the intracellular expression of COX-2 mRNA and protein (Fig. 2). Two-way ANOVA results revealed a significant difference between macrophages infected with IBV DMV/1639 and Conn A5968 strains in upregulation of COX-2 mRNA at 3, 6, and 12 hpi (Fig. 2a: treatments×time points versus control-non-treated and non-infected cells: $P<0.0001$). The data showed that infection with the IBV DMV/1639 strain induced about ten-fold higher COX-2 mRNA transcripts compared to infection with the IBV Conn A5968 strain or treatment with IFN-γ (100 ng $ml^{-1}$) in macrophages at 3 and 6 hpi (Fig. 2a: $P<0.0001$, and $P<0.0001$). In parallel, a quantitative assessment of intracellular COX-2 protein by a competitive ELISA in Fig. 3b demonstrated that levels of COX-2 protein were significantly higher in IBV-infected MQ-NCSU cells compared to non-treated and non-infected controls at all time points (Fig. 2b: $P<0.0001$, and $P<0.0001$). Similarly, the COX-2 protein level was elevated more than two-fold in IBV DMV/1639-infected MQ-NCSU than in mock control cells ($P<0.0001$). The efficacy of recombinant chicken IFN-γ was evaluated across a range of concentrations (0, 10, 100, 200, 250, 500, and 1000 ng $ml^{-1}$), revealing a significant inhibitory effect on cell viability at 250, 500, and 1000 ng $ml^{-1}$ (Fig. S2a). Subsequent analysis of COX-2 mRNA expression, normalized against the β-actin housekeeping gene, demonstrated that IFN-γ at 100 ng $ml^{-1}$ exhibited greater effectiveness compared to 250 ng $ml^{-1}$ (Fig. S2c). The images of confocal microscopy

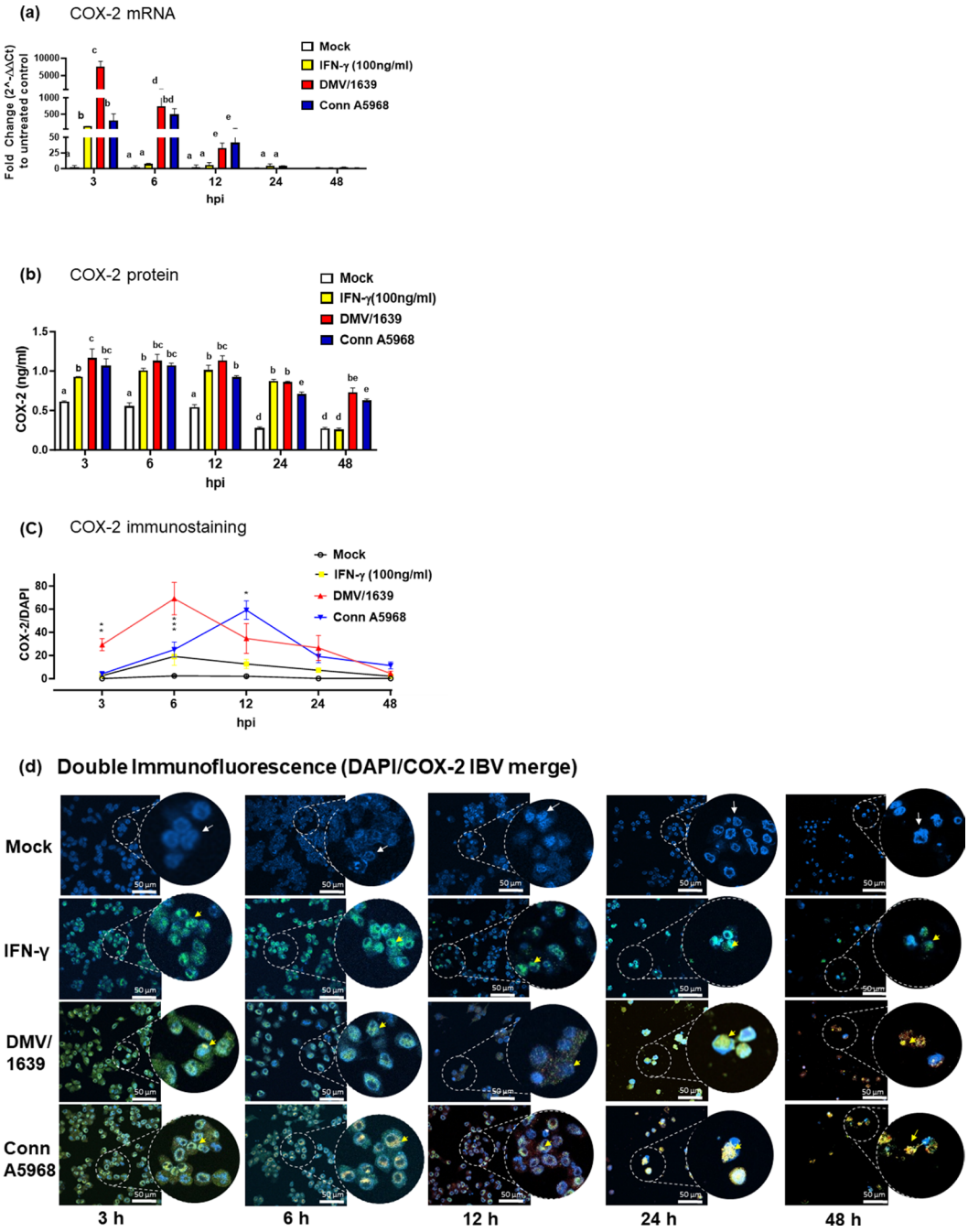


**Fig. 2.** Induction of expression of COX-2 following IBV infection of chicken macrophages. MQ-NCSU cells were seeded at $1.5\times10^6$ cells ml$^{-1}$ in 12-well culture plates and infected with IBV DMV/1639 or IBV Conn A5968 at an MOI of 0.1 along with IFN-γ (100 ng ml$^{-1}$)-treated and PBS-treated control cells. The expression of COX-2 mRNA was analysed by qPCR assay following total cellular RNA extraction and cDNA synthesis at indicated time points. The expressions of COX-2 mRNA (a) at indicated time points are illustrated. The expression of COX-2 mRNA was analysed by qPCR assay following total cellular RNA extraction and cDNA synthesis at 3, 6, 12, 24, and 48 hpi. The expressions of COX-2 mRNA (a) at indicated time points are illustrated. An ELISA kit was used for quantitative measurement of COX-2 protein in macrophage lysates at indicated time points (b). The immunofluorescence signals of COX-2 protein/DAPI in isotype control, IFN-γ (100 ng ml$^{-1}$)-treated, and IBV-inoculated cells (MOI=0.1) are quantified and illustrated in (c). The confocal images depict the double immunostaining of COX-2 protein and IBV-N antigen (d). At the indicated time points, the cell membranes were stained with a wheat germ agglutinin (10 µg ml$^{-1}$) conjugated to Alexa fluor 350 (blue in colour) for 30 min before being fixed with 4% cold paraformaldehyde and double-stained for IBV-N antigen and COX-2 protein that were visualized by Dylight 594 (IBV shown as red dots) and Dylight 488 (COX-2 shown as green dots), respectively. The merge of IBV-N antigen with COX-2 protein is shown as yellow dots. Nuclei were stained with the DAPI included in the anti-fade mounting medium. The white arrows indicate the cells, while the yellow arrows highlight the colocalization of IBV-N protein with COX-2 protein. The data in (d) represent one of two independent experiments. Two-way ANOVA followed by Bonferroni post-test were used for data analysis. Mean±SD values are accompanied by superscripts or asterisks when $P<0.05$.

in Fig. 2d depict COX-2 protein colocalization with IBV-N antigen in macrophages at all indicated time points. Analysis of normalized florescence signals of COX-2/DAPI under 60× power oil lenses was shown in Fig. 2c ($P$<0.0001, and $P$<0.0001). Taken together, these data suggest that IBV infection in macrophages induces the expression of COX-2 mRNA and protein.

### Inhibition of COX-2 expression decreases IBV infection in chicken macrophages

The selective COX-2 inhibitor SC-236 was used to further investigate the role of COX-2 expression in IBV infection in chicken macrophages. The impact of the selective COX-2 inhibitor SC-236 on macrophage viability was assessed at concentrations of 0, 5, 10, 20, 50, and 100 µg ml$^{-1}$, revealing a notable reduction in cell viability at concentrations ≥20 µg ml$^{-1}$ (Fig. S2c). Non-infected or IBV-infected macrophages were treated with SC-236 (10 µg ml$^{-1}$), and COX-2 protein levels were measured in equal amounts of cellular lysates at 3, 6, 12, and 24 hpi using the ELISA technique (Fig. 3b). Subsequent investigations focused on SC-236 concentrations of 5 and 10 µg ml$^{-1}$ to assess their inhibitory effects on IFN-γ (100 ng ml$^{-1}$)-induced COX-2 mRNA expression at 6 and 12 h post-treatments (Fig. S2d). Notably, the inhibitory effects of SC-236 on COX-2 mRNA expression were more pronounced at 10 µg ml$^{-1}$ compared to 5 µg ml$^{-1}$.

The data in Fig. 3c highlight a noteworthy reduction in COX-2 protein levels after treatment with SC-236 in IBV DMV/1639-infected macrophages at 3, 6, 12, and 24 hpi ($P$<0.0001). Similarly, SC-236 exerted significant inhibitory effects at all indicated time points in IBV Conn A5968-infected macrophages compared to in non-treated controls (Fig. 3b: $P$<0.0001, and $P$<0.0001 for treatment and time points, respectively). The dose-dependent effects of IFN-γ and SC-236 on macrophage viability was assessed by MTT assay (Fig. S2a and b). The maximum inhibitory dose of SC-236 was screened by RT-qPCR for COX-2 mRNA expressions at 6 h and 12 h after treatment of MQ-NCSU cells with IFN-γ (100 ng ml$^{-1}$) (Fig. S2c and d). The extension of the inhibitory effect of SC-236 on COX-2 production in IBV-infected MQ-NCSU cells was also confirmed by Western blot analysis and compared to non-treated and non-infected cells at 6 and 12 hpi (Fig. 3c).

To further investigate the effects of COX-2 reduction on IBV genome loads in chicken macrophages, IBV DMV/1639 and IBV Conn A5968-infected macrophages were treated with SC-236 (10 µg ml$^{-1}$) for 24 h, including untreated controls, and IBV genome

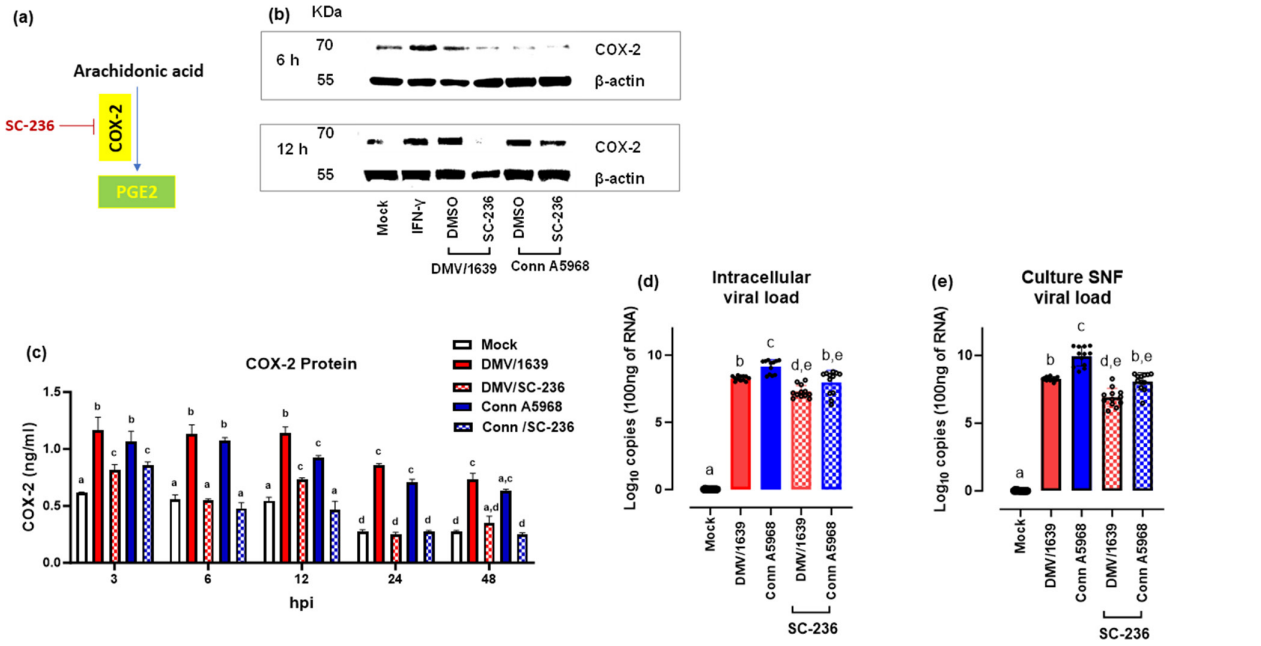


**Fig. 3.** Inhibition of COX-2 expression reduces IBV infection in chicken macrophages. (a) Schematic presentation outlines, the substrate (black), the metabolite (green box), the target enzyme (yellow box) and the inhibitor (red). MQ-NCSU cells infected with IBV-DMV/1639 or IBV Conn A5968 (MOI=0.1) were treated with a selective COX- inhibitor (SC-236 at 10 µg ml$^{-1}$) maintaining untreated controls. IBV-DMV/1639 or IBV Conn A5968-infected MQ-NCSU cells (MOI=0.1) were either treated with a selective COX-2 inhibitor (SC-236 at 10 µg ml$^{-1}$) maintaining untreated controls, and intracellular levels of COX-2 protein were visualized through Western blotting compared to IFN-γ (100 ng ml$^{-1}$)-treated and PBS-treated control cells. (b) Western blot analysis demonstrated COX-2 protein expression at 6 and 12 hpi against an internal control, β-actin. (c) Intracellular levels of COX-2 protein were quantified by ELISA at 3, 6, 12, 24, and 48 hpi. The data in (c) were analysed by two-way ANOVA followed by Bonferroni post-test for multiple comparisons. IBV genome loads were quantified in cells and culture supernatant fractions by qPCR following RNA extraction and cDNA synthesis. The data represents the Mean±SD of three independent experiments done in quadruplicate (d, e). The data in d and e were analysed by one way ANOVA followed by Bonferroni post-test. Values are indicated by a different superscript when $P$<0.05.

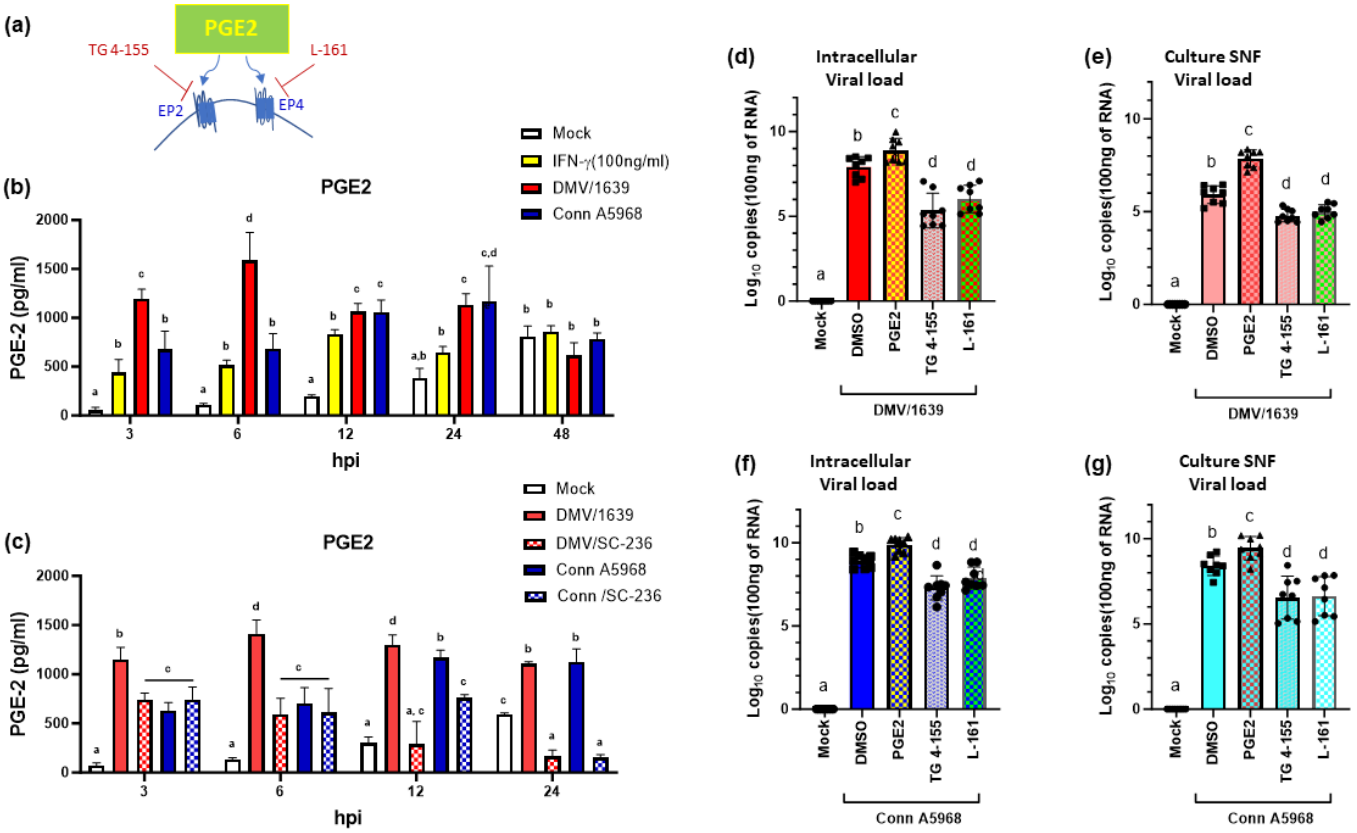


**Fig. 4.** Influence of PGE2 production on IBV infection in chicken macrophages. Schematic presentation in (a) illustrates PGE2 (in green box), two of its receptors PE2 and EP4 (blue), and their corresponding selective inhibitors (red). (b, c) The culture supernatant fluid (SNF) was collected from macrophages at 3, 6, 12, 24, and 48 hpi with IBV (MOI=0.1), compared to IFN-γ (100 ng ml$^{-1}$)-treated and PBS-treated control cells. PGE2 in the culture SNF was quantified by an ELISA technique. Two-way ANOVA Bonferroni post-test revealed significant increases of PG2 production at 3, 6, 12, and 24 hpi following IBV infection of macrophages (b). PGE2 production was reduced by treatment with a selective COX-2 inhibitor (SC-236:10 µg ml$^{-1}$) (c). (d–g) After 1 h adsorption with IBV, infected MQ-NCSU cells were either 24 h-treated or not with exogenous PGE2 (5 µg ml$^{-1}$), EP2 and EP4 receptors inhibitors TG4-155 (4 µM) and L-161 (8 µM), respectively, and viral genome loads were quantified in macrophages and culture SNF by q-PCR following RNA extraction and cDNA synthesis at 24 hpi with IBV. Data in (d–g) were analysed by one-way ANOVA followed by Bonferroni post-test, and represent the mean±SD of three separate experiments, and all samples were run in quadruplicates. Significant differences are indicated by asterisks or superscripts when $P$<0.05.

loads were measured in cells and in cell culture supernatant fractions (Fig. 3d, e). The data presented in Fig. 3d, e demonstrate a substantial decrease in IBV genome loads in cells treated with SC-236 compared to non-treated control cells at 24 hpi, regardless of the IBV strain (DMV/1639 or Conn A5968; $P$<0.0001). A similar trend was observed in Fig. 3e, with $P$<0.0001. Taken together, these results indicated that the antagonism of COX-2 production reduces IBV replication in macrophages.

## Influence of PGE2 production on IBV infection in chicken macrophages

In order to investigate the consequences of enhanced COX-2 production in IBV-infected macrophages, the active metabolic product of COX-2 activity PGE2 was measured in culture supernatants at 3, 6, 12, 24, and 48 hpi using an ELISA assay (Fig. 4b). The outcomes in Fig. 4b reveal a significant increase in PGE2 release in the culture supernatant of macrophages infected with IBV at 3, 6, 12, and 24 hpi compared to controls ($P$=0.0024 for time points, and $P$<0.0001 for treatments). Non-infected cells were simultaneously treated with IFN-γ (100 ng ml$^{-1}$) as a positive control. Consistently, IBV DMV/1639-infected macrophages showed higher PGE2 production than those infected with IBV Conn A5968 strain at 3 and 6 hpi ($P$=0.003, $P$<0.0001, respectively). However, no significant differences were observed between infected and non-infected control cells at 48 hpi ($P$>0.05). Furthermore, we studied the effect of selective COX-2 inhibitor SC-236 on PGE2 release in IBV-infected macrophages at 3, 6, 12, and 24 hpi. The findings in Fig. 4c indicated an augmented production of PGE2 in IBV DMV/1639 or Conn A5968-infected macrophages, a response significantly attenuated by treatment with the selective COX-2 inhibitor SC-236 (10 µg ml$^{-1}$) at the specified time points ($P$=0.02 for time points, and $P$<0.0001 for treatments). Taken together, these data indicate that IBV infection increases PGE2 release through COX-2 production in MQ-NCSU cells in a time- and strain-dependent manner.

Because PGE2 release was considered a vital metabolic product of COX-2 activity, and PGE2 was increased in the IBV-infected macrophages, we further investigated its role on IBV genome loads. IBV DMV/1639 or IBV Conn A5968-infected macrophages were exposed to 24 h treatment with exogenous PGE2 (5 μg ml$^{-1}$). An initial assessment of the dose-dependent impact of PGE2 on macrophage viability was conducted through a 24 h MTT assay (Fig. S3a). The percentage of cell viability in DMSO-treated control cells was established as 100%, and all drug-treated cell viabilities were normalized accordingly. The results indicated a minimum inhibitory concentration of 20 μg ml$^{-1}$ on cell viability, whereas the dose employed in the present study was 5 μg ml$^{-1}$. The results illustrated in Fig. 4d demonstrate a remarkable elevation in IBV DMV/1639 genome loads after 24 h of PGE2 treatment compared to non-treated cells ($P$<0.001). Similarly, the inhibitory effects of EP2 inhibitor (TG4-155) and EP4 inhibitor (L-161) were dose-dependent, resulting in declines in cell viability at concentrations of 16 μM (Fig. S3b and c). This led to further investigations at lower concentrations, ensuring a comprehensive understanding of the dose-response relationship.

A similar pattern was observed in Fig. 4e, with $P$<0.0001. Furthermore, we studied the IBV genome loads after antagonizing the PGE2 (EP) receptors in IBV DMV/1639-infected macrophages. Concurrently, the results from the analysis of Fig. 4d–g indicate that the 24 h treatment of IBV DMV/1639-infected MQ-NCSU cells with selective EP2 and EP4 receptors inhibitors, TG 4–155 (4 μM) and L-161 (8 μM), respectively, significantly diminished the IBV DMV/1639-genome loads in both cell and culture supernatant fractions ($P$<0.0001 for Fig. 4d and $P$=0.0013 for Fig. 4e). The dose-dependent impacts of these inhibitors on MQ-NCSU cell viability were exhibited at micromolar concentrations (refer to Fig. S3b and c), with the doses employed in this experiment representing half of the inhibitory concentration on cell viability. The observed effects for EP2 and EP4 receptors inhibitors on IBV DMV/1639-infected macrophages were also reproduced in IBV Conn A5968 strain (Fig. 4f, $P$=0.015, and Fig. 4g, $P$<0.0001). To sum, these results suggested that IBV-genome loads were suppressed by chemical inhibitors of COX-2, PGE2 receptor antagonists; EP2 and EP4 inhibitor. To investigate the effect of one of the upstream signalling of COX-2 synthesis, we used the selective chemical inhibitors to JAK-1 and JAK-II 420099 (15 nM) and SP600125 (40 nM), respectively, in IBV-infected macrophages (Fig. 4d, e). The dose-dependent effects of JAK-I inhibitor (420099) and JAK-II inhibitor (SP600125) were explored at concentrations ranging from 0 to 100 μM, respectively, (Fig. S3d and e). The inhibitory effects revealing declines in cell viability at 3 μM and 10 μM (Fig. S3d and e, respectively). Consequently, subsequent investigations were conducted at lower concentrations to delineate the intricate details of the observed inhibitory effects. The 24 h treatment of IBV DMV/1639 and IBV Conn A5968-infected MQ-NCSU cells with the JAK-II inhibitor SP600125 (40 nM) led to a significant reduction in viral genome loads within the cells, as revealed by statistical analysis (Fig. 4d, f: $P$=0.0027, $P$<0.0001) and in the culture supernatant (Fig. 4e, g: $P$<0.0021, $P$=0.0006) as well. But such significant effects on IBV-genome loads were not found in case of 24 h treatment with JAK-I inhibitor 420099 (15 nM), either intracellularly (Fig. 4d, f) or extracellularly (Fig. 4e, g). In summary, these results suggested that IBV-genome loads were suppressed by chemical inhibitors of COX-2, PGE2 receptor antagonists EP2 and EP4 and by JAK-II inhibitor.

In Fig. 5 (a–b), our findings reveal a significant impact of IBV DMV/1639 strains on PGE2 production in macrophages compared to non-infected controls (Fig. 4a). This effect is not observed with the IBV Conn A5968 strain (Fig. 4b). Additionally, 24 h treatments with IFN-γ significantly increase PGE2 release compared to mock treatments, and this effect is not observed in the case of Conn A5968-infected cells. However, the treatment of infected cells with the JAK-I inhibitor (420099; 15 nM) robustly increases PGE2 release in both strains, and this effect is not observed after JAK-II treatment (SP600125; 40 nM).

Furthermore, a 30 min pretreatment with the JAK-1 inhibitor, followed by IFN-γ after IBV infection, mitigates the observed increase in PGE2 production (Fig. 4a, b). While a 24 h treatment of IBV-infected cells with the JAK-II inhibitor is associated with a reduction in PGE2 release compared to non-treated cells, a 30 min pretreatment of IFN-γ-treated and infected macrophages is linked to a recovery in PGE2 production.

In Fig. 5 (c–d), our results demonstrate potent inhibitory effects of IFN-γ on IBV genome loads, observed both intracellularly and in the culture supernatant. To assess the activation of the JAK-STAT pathway by IFN-γ in IBV-infected chicken macrophages, we utilized pharmacological antagonists targeting JAK-1 or JAK2. Exploring the impact of upstream signalling on COX-2 synthesis, we employed selective chemical inhibitors for JAK-1 and JAK-II: 420099 and SP600125, respectively, in IBV-infected macrophages (see Fig. 4d, e). The impact of these inhibitors on MQ-NCSU cell viability was illustrated in micromolar concentrations, and the chosen doses for 420099 (15 nM) and SP60025 (40 nM) were well within a safe range, as demonstrated in Fig. S3d and e. The analysis outcomes revealed that the 24 h treatment of IBV DMV/1639 and IBV Conn A5968-infected MQ-NCSU cells with the JAK-II inhibitor SP600125 (40 nM) resulted in a significant reduction in viral genome loads within the cells ($P$=0.0027 for Fig. 5d, $P$<0.0001 for Fig. 5f) and in the culture supernatant ($P$<0.0021 for Fig. 4e, $P$=0.0006 for Fig. 4g). However, such noteworthy effects on IBV genome loads were not observed with a 24 h treatment of the JAK-I inhibitor, 420099 (15 nM), either intracellularly (Fig. 5d, f) or extracellularly (Fig. 5e, g). These observations contribute valuable insights into the intricate regulatory mechanisms underlying IFN-γ responses in IBV-infected chicken macrophages. Taken together, the previous findings suggested that IBV-genome loads were suppressed by chemical inhibitors of COX-2, PGE2 receptor antagonists; EP2 and EP4, and by JAK-II inhibitor.

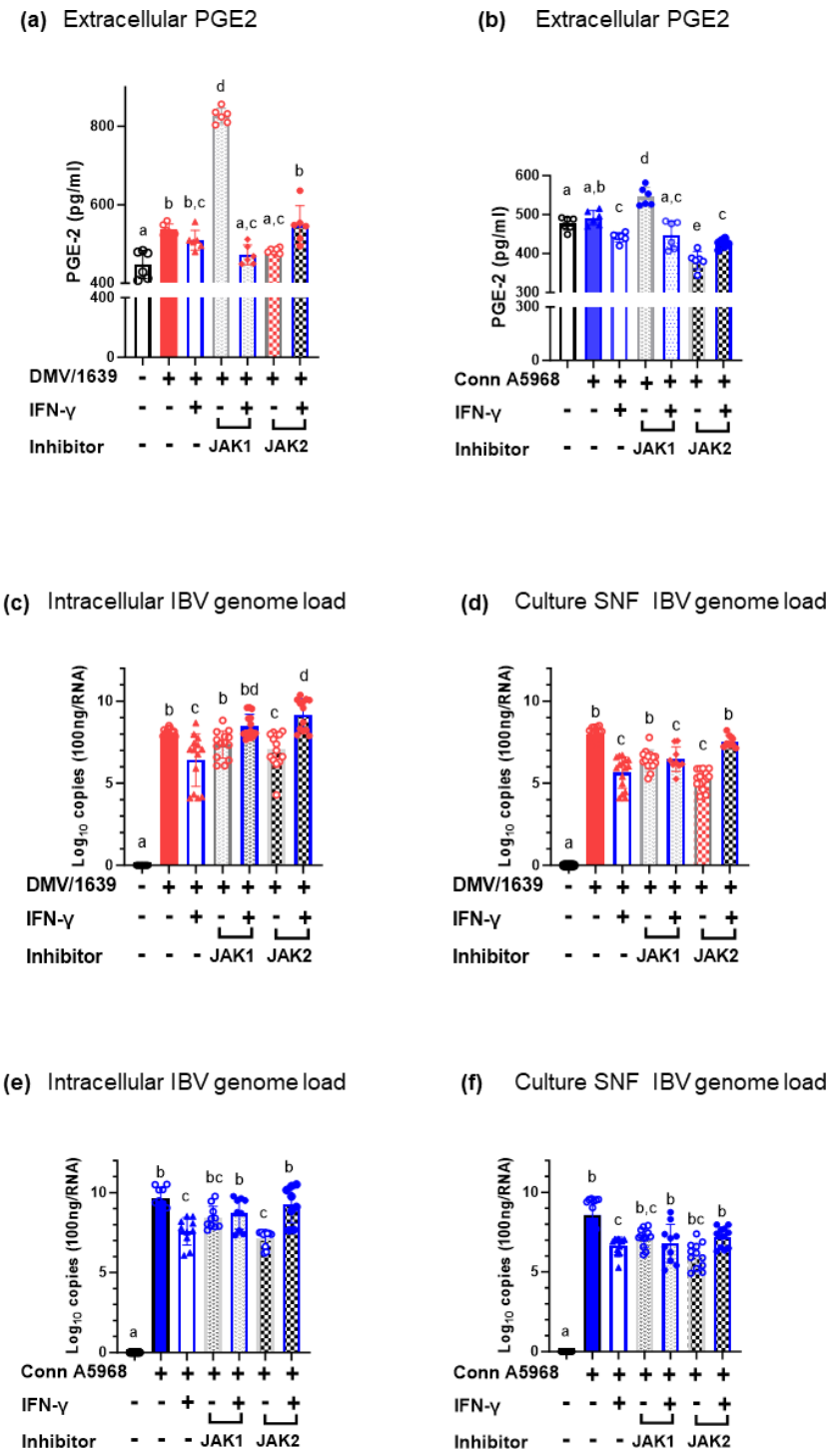


**Fig. 5.** Impact of IFN-γ treatment and pharmacological inhibition of Janus Kinases (JAK) on PGE2 production and IBV infection in chicken macrophages. Following IBV adsorption (MOI=0.1), MQ-NCSU cells were subjected to a 24 h treatment with IFN-γ (100 ng ml$^{-1}$) and JAK-I and JAK-II inhibitors; 420099 (15 nM) and SP600125 (40 nM), respectively, or left untreated. Subsequently, the culture supernatant fluid (SNF) was collected, and PGE2 levels were quantified using an ELISA technique. Significant increases in PGE2 production at 24 hpi were observed following IBV infection of macrophages in DMV/1639 (a) but not after Conn A5968 strains (b), as revealed by a one-way ANOVA Bonferroni post-test. The data in (a) and (b) are derived from two independent experiments, with each experiment represented in ELISA by triplicates. PGE2 production was measured after treatment with 420099 (15 nM) and SP600125 (40 nM), respectively (c, f). Viral genome loads were quantified at 24 hpi in both macrophages and culture SNF using q-PCR after RNA extraction and cDNA synthesis (d-g). Data were analysed using one-way ANOVA followed by Bonferroni post-test. The results in (d-g) represent the mean±SD of three independent experiments, with all samples run in quadruplicate. Significant differences are denoted by asterisks or superscripts when $P$<0.05.

### Influence of IBV infection and COX-2/PGE2 pathway on NO production in chicken macrophages

To assess the impact of IBV-induced activation of the COX-2/PGE2 pathway on one of the macrophage host defence mechanisms, measurements of NO production were conducted, evaluating iNOS mRNA expression and its active metabolite $NO_2$ levels after IBV infection. The results obtained from the experimental interventions across five distinct time points revealed a noteworthy upregulation in iNOS mRNA expression in IBV DMV/1639 and Conn A5968-infected macrophages at 6 hpi (Fig. 6a, $P<0.012$, $P=0.011$, respectively). This increase in iNOS mRNA expression subsequently translated into heightened concentrations of $NO_2$ in both viral strains at 12, 24, and 48 hpi (Fig. 6b, $P<0.0001$). Likewise, the selective COX-2 inhibition with SC-236 (10 µg ml$^{-1}$) demonstrated substantial inhibitory effects on iNOS mRNA expression at 24 hpi in DMV/1639 – but not for IBV Conn A5968-infected macrophages compared to in untreated controls (Fig. 6c: $P<0.0001$, $P<0.042$, respectively). Furthermore, a consistent inhibitory effect on $NO_2$ concentration was observed when selective COX-2 inhibition (SC-236) was used in IBV-infected cells compared t controls (Fig. 5d: $P<0.0001$, $P<0.0001$).

Furthermore, we investigated the influence of selective inhibitors targeting EP2, EP4, JAK-I, and JAK-II on iNOS mRNA expression (Fig. 6e, g) and NO2 release (Fig. 6f, h) in IBV-infected macrophages at 24 hpi. The results of the statical analysis revealed a significant decrease in iNOS mRNA expression, coupled with reduced NO release in the culture supernatant of both IBV DMV/1639 and Conn A5968-infected and inhibitor-treated macrophages, compared to their infected, non-treated counterparts (Fig. 6e, g; $P<0.0001$ for iNOS mRNA expression, Fig. 6f, h; $P<0.0001$ for NO production). Concurrently, exposure to PGE2 (5 µg ml$^{-1}$) for a duration of 24 h markedly mitigated both iNOS mRNA expression and NO2 release in IBV DMV/1639 and IBV Conn A5968-infected macrophages (Fig. 6e, g: $P<0.0001$, $P<0.0001$, respectively). Notably, the suppressive effects of PGE2 on iNOS mRNA expression in IBV Conn A5968- and NO2 release in DMV/1639-infected cells were found to be statistically insignificant (Fig. 6e, h: $P>0.05$). Furthermore, the conspicuous inhibitory impacts observed with the selective COX-2 inhibitor SC-236, exogenous PGE2 treatment, selective PGE2 receptor blockers (EP2, EP4), JAK-I, and JAK-II inhibitors on both iNOS mRNA expression and NO2 concentrations (Fig. 6e–h, $P<0.0001$) provide valuable insights into potential targets for modulating host defence responses in IBV-infected macrophages.

### Influence of IBV infection and COX-2/PGE2 pathway on IL-6 mRNA expression in chicken macrophages

A substantial surge in IL-6 mRNA expression was observed, particularly at 3 hpi following infection with IBV DMV/1639 and IBV Conn A5968 strains (Fig. 7a, $P<0.0001$), and persisting the increase at 6 hpi (Fig. 7a, $P<0.0001$). Administration of the selective COX-2 inhibitor SC-236 (10 µg ml$^{-1}$) demonstrated marked inhibitory effects on IL-6 mRNA expression at 24 hpi in both IBV DMV/1639 and IBV Conn A5968-infected macrophages, as compared to untreated and infected controls (Fig. 7b, $P<0.0001$, $P<0.0001$).

The inhibitory impact of EP2 and EP4 receptor antagonists on IL-6 mRNA expression in IBV DMV/1639-infected macrophages was consistently reproduced in the IBV Conn A5968 strain. Similarly, the administration of selective chemical antagonists for JAK-I and JAK-II, namely 420099 (15 nM) and SP600125 (40 nM) respectively, elicited comparable inhibitory effects in both IBV DMV/1639 and IBV Conn A5968-infected macrophages (Fig. 7c, d; $P<0.0001$, $P<0.0001$, respectively). In contrast, exogenous PGE2 demonstrated an enhancing effect on IL-6 mRNA expression in IBV-infected macrophages (For IBV DMV/1639 and IBV Conn A5968, the *P*-values were both <0.0001; Fig. 7c, d). These findings underscore the upregulation of IL-6 expression during IBV infection, with EP2, EP4 receptors, JAK-I, and JAK-II pathways playing crucial roles in IL-6 mRNA modulation. Additionally, the impact of exogenous PGE2 highlights the multifaceted nature of host-virus interactions in IBV-induced immune response.

## DISCUSSION

The study was conducted to investigate the effect of IBV infection of chicken macrophages on the synthesis of COX-2 and its main metabolite, PGE2, and to explore the consequences of COX-2 and PGE2 induction on IBV replication. Moreover, we investigated the effect of modulation of the COX-2/PGE2 pathway on the IBV infection in macrophages and the expression of pro-inflammatory mediators such as NO and IL-6. In our study, we observed that IBV significantly elevates the production of COX-2, both in terms of mRNA and protein levels, within chicken macrophages. Subsequently, treatment with a specific COX-2 antagonist effectively suppressed COX-2 synthesis and the release of PGE2. Furthermore, when IBV-infected MQ-NCSU cells were subjected to treatment with COX-2 inhibitor PGE2 receptors blockers (EP2 and EP4), or JAK-II inhibitor, we observed a notable reduction in both intracellular and extracellular loads of the IBV genome as well as the expression of pro-inflammatory mediators (NO and IL-6). We also observed that IBV infection increases the expression of NO and IL-6 in chicken macrophages. These findings strongly suggest a significant role of COX-2/PGE2 signalling in the replication of IBV and modulation of pro-inflammatory signalling. Our findings contribute to a better understanding of the chicken macrophage–IBV interaction and establish check points for intervention to decrease IBV infection in macrophages.

Chicken macrophages play a pivotal role during IBV infection. Not only does IBV target macrophages *in vitro* and *in vivo* for replication, but it also alters the host responses induced by macrophages [10, 46]. Previous studies examining IBV replication in avian macrophages reveals strain-dependent responses. For instance, Sun *et al.* [41] and Han *et al.* [47] demonstrated successful

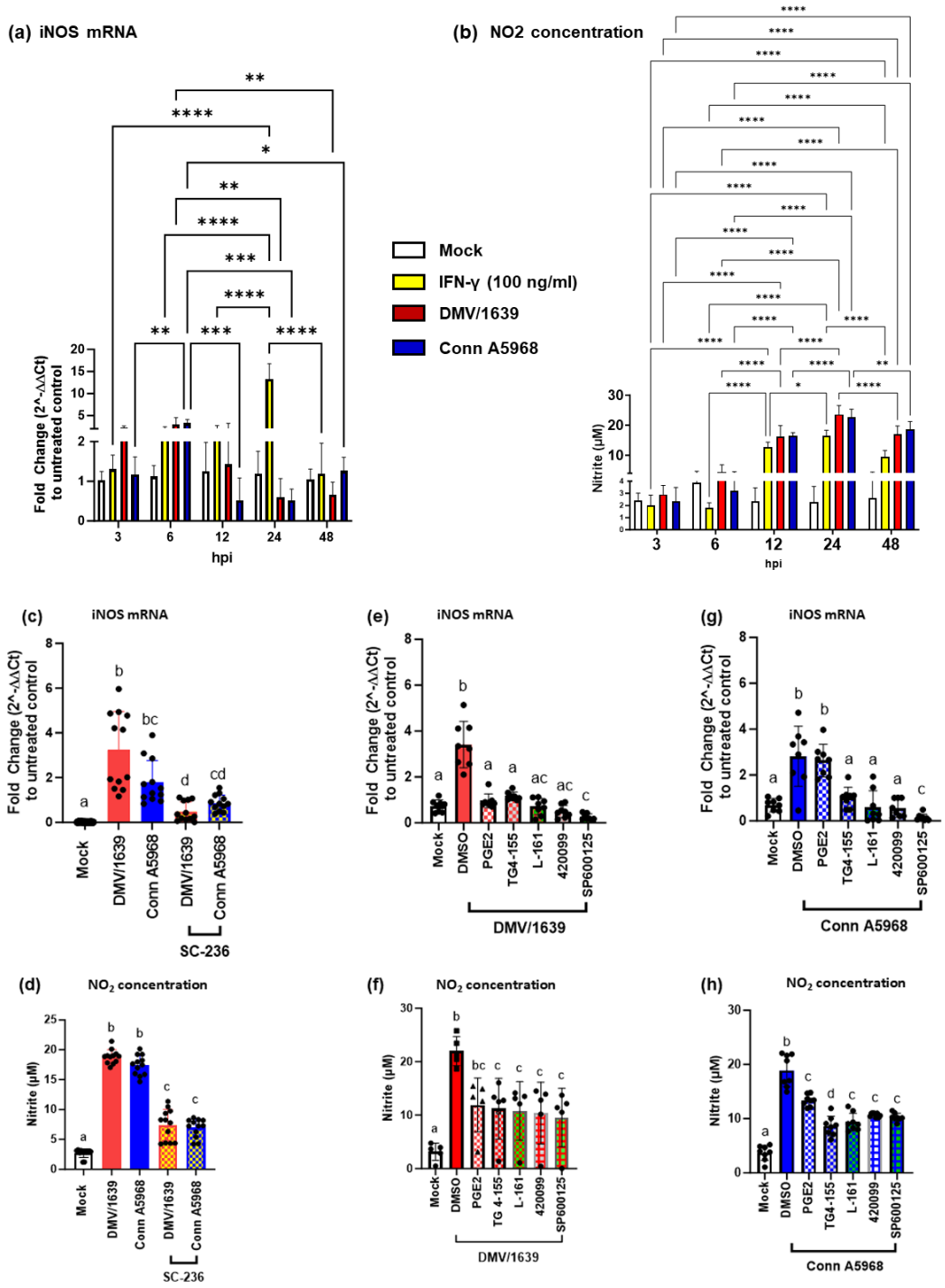


**Fig. 6.** Influence of IBV infection and the COX-2/PGE2 pathway on NO production in chicken macrophages. Quantification of iNOS mRNA and NO active metabolite NO2 in IBV-DMV/1639 or IBV Conn A5968-infected MQ-NCSU cells (MOI=0.1) treated with IFN-γ (100 ng ml$^{-1}$) as a positive control, and PBS-treated cells. Macrophages and culture supernatants were collected at 3, 6, 12, 24, and 48 hpi (a, b). The data, analysed using two-way ANOVA Bonferroni post-test, represent two independent experiments with all samples run in triplicate. After 1 h of adsorption with IBV, MQ-NCSU cells were treated or not for 24 h with exogenous PGE2 (5 µg ml$^{-1}$), EP2 and EP4 receptors inhibitors (TG4-155, 4 µM, and L-161, 8 µM, respectively), or JAK-I and JAK-II inhibitors (420099, 15 nM, and SP600125, 40 nM, respectively) (d–g), while maintaining DMSO-treated controls (c-h). iNOS mRNA and NO2 were measured at 24 hpi. The data in (c, d) are from three independent experiments, with all samples run in quadruplicate, while those in (e, h) are from two independent experiments, with all samples run in quadruplicate. Data were analysed by one-way ANOVA Bonferroni post-test, and values are accompanied by superscripts when $P$<0.05.

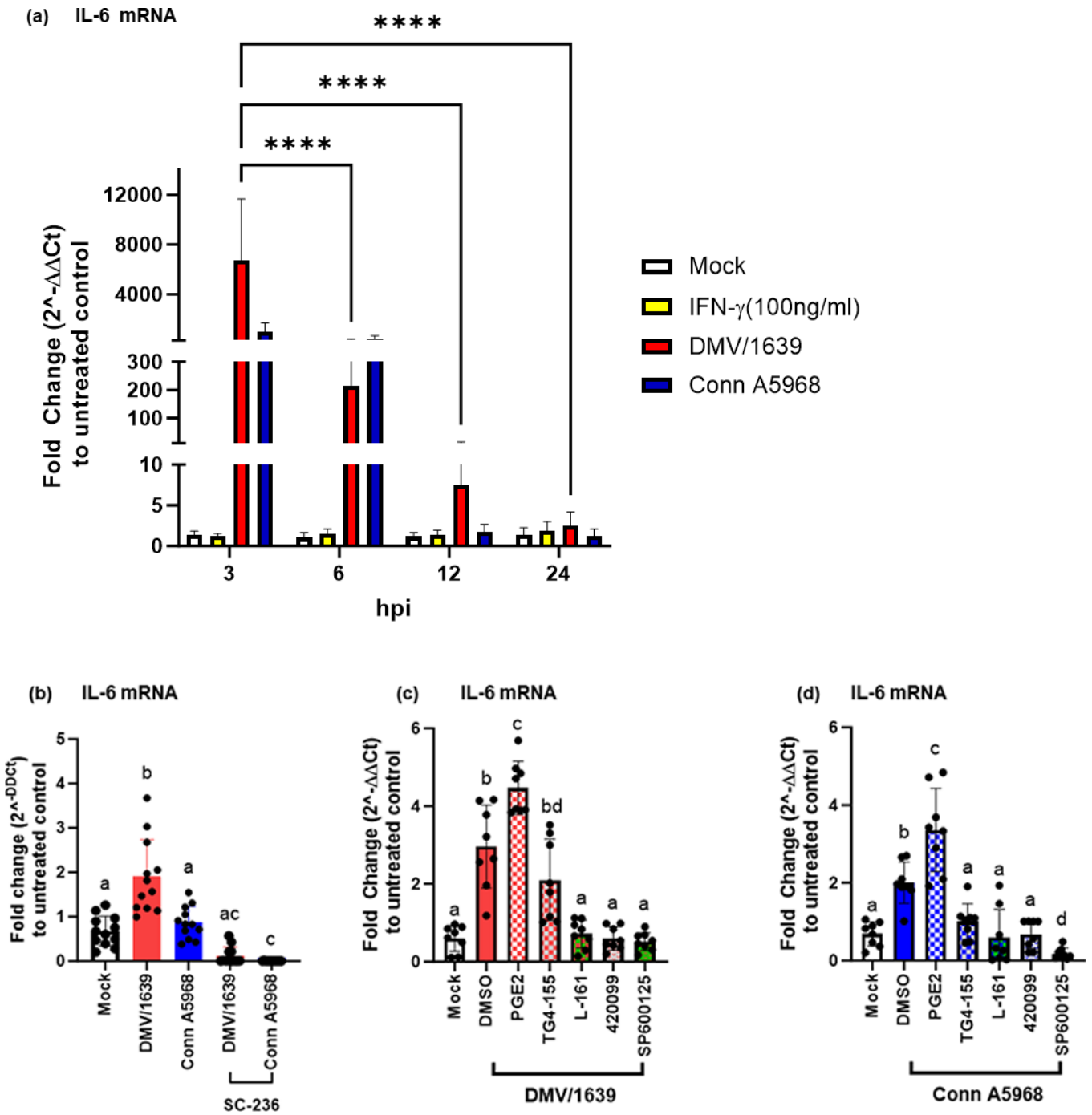


**Fig. 7.** Influence of IBV infection and pharmacological inhibition of COX-2/PGE2 and Janus kinases (JAK) on IL-6 mRNA expression in chicken macrophages. IL-6 mRNA expression was assessed in MQ-NCSU cells infected with IBV-DMV/1639 or IBV Conn A5968 at an MOI=0.1, collected at 3, 6, 12, 24, and 48 hpi, in comparison to IFN-γ (100 ng ml$^{-1}$)-treated and PBS-treated control cells (a). The data in (a) are from two independent experiments, subjected to analysis through two-way ANOVA and Bonferroni post-test, with all samples executed in triplicates. (b–d) Following 1 h adsorption with IBV, infected MQ-NCSU cells were either treated or untreated for 24 h with a selective COX-2 antagonist (SC-236 at 10 µg ml$^{-1}$), exogenous PGE2 (5 µg ml$^{-1}$), EP2 and EP4 receptors inhibitors (TG4-155 at 4 µM and L-161 at 8 µM, respectively), or inhibitors of JAK-I and JAK-II (420099 at 15 nM and SP600125 at 40 nM, respectively), while maintaining DMSO-treated controls (b-d). IL-6 mRNA expression was evaluated at 24 hpi. The data presented in (b) are from three independent experiments, with all samples analysed in quadruplicates, while those in (c,d) are from two independent experiments, with all samples analysed in quadruplicates. Statistical analyses were performed using one-way ANOVA Bonferroni post-test, and values are denoted by superscripts when $P<0.05$.

replication of IBV strain M41 in chicken macrophage cell line HD11, accompanied by upregulated expression of IFN-α, IL-1β, and IL-6 [41, 47]. Amarasinghe *et al.* [10] observed replication of M41 and Conn A5968 IBV strains in macrophages, leading to modulation of macrophage responses. In agreement with previous observations, in our investigations, we observed robust IBV replication in avian macrophages, with notable differences between IBV strains DMV1639 and Conn A5968.

First, IBV as a single-stranded RNA virus may trigger a series of signalling pathways in chicken macrophages following infection [31, 32, 36], but its role in triggering a COX-2/PGE2 pathway in macrophages is still unclear. The IBV can induce expression of various immune receptors, including TLRs [32], which recognize viral components. Activation of these receptors initiates intracellular signalling cascades that culminate in the upregulation of COX-2 gene expression [9, 10]. It is pertinent to note that IBV inoculation of chickens led to an increase in COX-2 mRNA expression within the spleen and thymus, as reported in a recent study [29]. Additionally, in mature chickens, IBV infection elicited heightened levels of both COX-2 mRNA expression and PGE2 production in the uterine mucosa [24]. Although the role of the COX-2/PGE2 pathway during IBV infection is not known, this pathway has been shown to suppress the immune response to mammalian viral infections, such as herpes simplex virus, rotavirus, influenza A virus, human immunodeficiency virus (HIV) [11–13], and avian viruses, such as MDV [27, 28].

In the current study, we found that selective COX-2 antagonist SC-236, 4-[5-(4-chlorophenyl)-3-(trifluoromethyl)-1-pyrazol-1-l] benzenesulfonamide [48, 49], has inhibitory effects on both COX-2 production and viral genome loads in IBV-infected chicken macrophages with both strains of IBV: DMV/1639 and Conn A5968. By blocking COX-2 activity, these antagonists can effectively reduce the production of PGE2, which is synthesized by COX-2 [16]. Consequently, the selective COX-2 antagonist would be expected to decrease COX-2 production in IBV-infected chicken macrophages due to their well-investigated inhibitory action on nuclear factor kappa B (NF-κB) [19]. COX-2-derived PGE2 has been shown to modulate immune responses during viral infections [21]. In the current study, by inhibiting COX-2 by using selective COX-2 antagonists can alter the balance of pro-inflammatory and anti-inflammatory mediators during IBV replication, as has been seen for gamma herpesvirus mediated tumorigenesis [49]. The observed action of COX-2 inhibitor SC-236, may be attributed to its suppressive influence on NF-κB activation, as well as the phosphorylation of p38 mitogen-activated protein kinase (MAPK), extracellular signal-regulated kinase, and c-Jun N-terminal kinase. This mechanism, illustrated in human mast cell line cells, extends beyond COX-2 specificity, affecting the expression of TNF-α, IL-6, IL-8, vascular endothelial growth factor, COX-2, and iNOS in such cells [49], as well as in murine fibroblast cells [50, 51]. Moreover, this antagonistic effect on NF-κB was consistently observed in the chicken macrophage cell line [52].

The reversal of impact of treatment with exogenous PGE2 treatment on IBV replication has been validated by using pharmacological inhibitors to EP2 and EP4 receptors, TG4-155 and L1-161, respectively (Fig. 4c–f). Furthermore, the rescue effects of IFN-γ on IBV replication has been reversed by 30 min treatment with JAK-II antagonist SP60025 (Fig. 5c–f). The downstream signalling of COX-2 production leads to PGE2 production, and that exerts significant biological activities through PGE2 receptors EP2 and EP4 in chickens [26–28] and mammals [20]. Since EP1 receptors in chickens have not been identified so far, in the current study, the selective chemical antagonists of PGE2 receptors (EP) targeting EP2 and EP4 were applied to examine the role of PGE2 in IBV-infected macrophages. Our results showed that blocking of both EP2 and EP4 significantly reduced the intracellular and extracellular viral genome loads in IBV-infected macrophages. Therefore, it is likely that the COX-2/PGE2 pathway, particularly PGE2, influences the viral genome load of IBV-infected chicken macrophages.

Our study demonstrated that JAK–II inhibitor SP600125 is capable of reduction of IBV-genome loads both intracellularly and in the culture supernatant of IBV-infected macrophages. An effect was noticed in both IBV strains, though such an effect was not observed in the case of treatment with JAK-I inhibitor 420092, and this is difficult to explain. Overall, our data indicated that inhibition of JAK-II decreases the IBV loads in macrophages, and our observation in this regard agrees with the observations made on other host viral models involving SARS-CoV-2, and Middle East respiratory syndrome coronavirus (MERS-CoV) [53, 54].

Our results in Fig. 5 highlights the distinctive impact of IBV DMV/1639 strains on PGE2 production in macrophages, contrasting with the negligible effect observed in the IBV Conn A5968 strain. Additionally, the heightened PGE2 release following 24 h IFN-γ treatments is specific to non-mock conditions, as Conn A5968-infected cells do not exhibit this response. Notably, the JAK-I inhibitor (420099; 15 nM) significantly amplifies PGE2 release in both IBV strains, while JAK-II treatment (SP600125; 40 nM) fails to induce a similar effect. Furthermore, our study reveals that a 30 min pretreatment with the JAK-1 inhibitor, followed by IFN-γ post-IBV infection, effectively attenuates the observed increase in PGE2 production (Fig. 4a, b). Conversely, a 24 h treatment with the JAK-II inhibitor in IBV-infected cells leads to a reduction in PGE2 release, yet a 30 min pretreatment of IFN-γ-treated and infected macrophages results in a notable recovery in PGE2 production. These nuanced responses underscore the complex interplay between IBV strains, interferon signalling, and JAK inhibition in regulating PGE2 dynamics in macrophages.

In Fig. 5 (c–f), our study unveils the potent inhibitory influence of IFN-γ on IBV genome loads, both intracellularly and in the culture supernatant. To unravel the involvement of the JAK-STAT pathway triggered by IFN-γ in IBV-infected chicken macrophages, we employed pharmacological antagonists targeting JAK-I or JAK-II. By using selective chemical inhibitors for JAK-I and JAK-II – 420099 and SP600125, respectively – in IBV-infected macrophages (refer to Fig. 4d, e), we assessed their impact on upstream signalling and COX-2 synthesis. The chosen doses for 420099 (15 nM) and SP60025 (40 nM) were well within a safe range, as illustrated in Fig. S3d and e, depicting the effect of these inhibitors on MQ-NCSU cell viability.

Intriguingly, such noteworthy effects on IBV genome loads were not observed with a 24 h treatment of the JAK-I inhibitor, 420099 (15 nM), either intracellularly (Fig. 5d, f) or extracellularly (Fig. 5e, g). These observations contribute valuable insights into the intricate regulatory mechanisms governing IFN-γ responses in IBV-infected chicken macrophages, shedding light on the potential therapeutic avenues for modulating viral replication dynamics.

Our results demonstrate a notable increase in iNOS mRNA expression and elevated concentrations of NO, particularly in IBV DMV/1639-infected macrophages at certain time points. The use of exogenous PGE2 treatment and PGE2 receptor antagonists (EP2, EP4) indicated that iNOS mRNA expression and NO concentrations are induced downstream of PGE2 production, highlighting the regulatory role of the COX-2/PGE2 pathway in the context of IBV-induced immune responses. PGE2 has demonstrated an ability to elevate viral genome load, and reciprocally viral infection has been shown to increase the cellular PGE2 release [21], an effect that was associated with reduced NO production [39, 55].

The observed significant surge in IL-6 mRNA expression following IBV infection aligns with previous studies of Sun *et al.* [41], which consistently highlighted a substantial upregulation of various pro-inflammatory genes, including IL-6, in IBV-infected chicken macrophages. The use of exogenous PGE2 treatment and PGE2 receptor antagonists (Ep2, EP4) indicated that IL-6

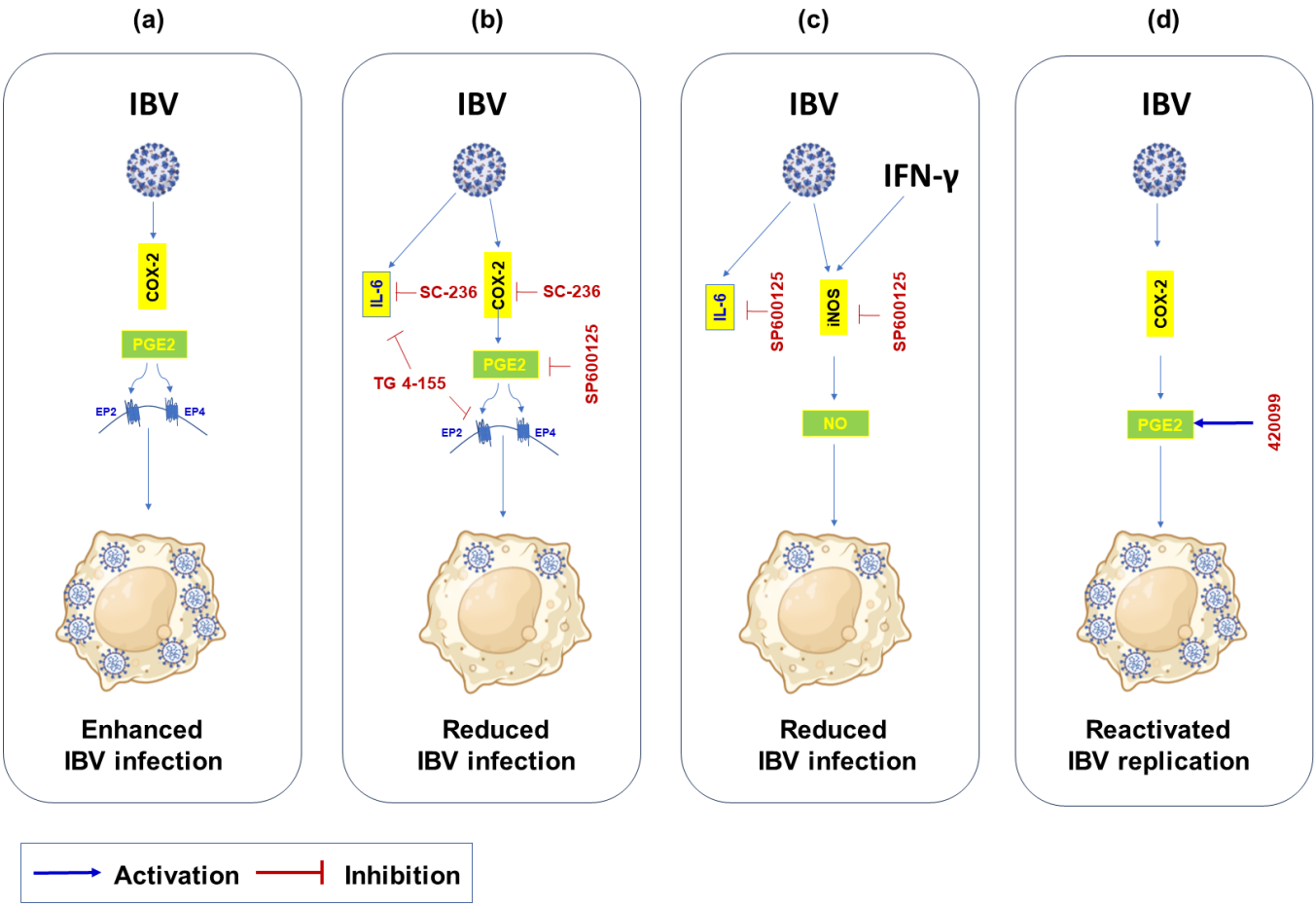


**Fig. 8.** Model of COX-2/PGE2 activation and pharmacological inhibition in IBV-infected chicken macrophages. A schematic representation illustrating the systematic modulation of the COX-2/PGE2 pathway by IBV in avian macrophages. Upon IBV infection, macrophages undergo upregulation of COX-2 synthesis, resulting in increased production and release of PGE-2 (a). Pharmacological intervention with a selective COX-2 inhibitor, SC-236, leads to a reduction in both PGE-2 production and IBV-genome load (b). Conversely, exogenous PGE2 treatment exacerbates IBV load, while inhibition via chemical inhibitors targeting PGE2 receptors (EP2) or JAK-II mitigates viral genome loads (c). Whereas treatment of the infected cells with JAK-I (420099) inhibitor was associated with enhanced PGE2 release and reactivation of infection (d). Solid blue arrows signify activation, and dashed grey arrows signify inhibition. This schematic serves as a model portraying the intricate interplay of COX-2/PGE2 pathways during IBV infection in avian macrophages. The depicted pathways involve well-established molecular components, and directional arrows signify activation or inhibition processes. Abbreviations; IBV; infectious bronchitis virus, COX-2; cyclooxygenase-2, PGE2; prostaglandin E2, IL-6; interleukin-6, iNOS; inducible nitric oxide synthase, NO; nitric oxide.

mRNA is induced downstream of PGE2 production, highlighting the regulatory role of the COX-2/PGE2 pathway, particularly PGE2 in the context of IBV-induced immune responses.

Based on the findings of the current study and the observations of others [32, 41, 46, 47], we propose the model of induction of COX-2/PGE2 and pro-inflammatory mediators as illustrated in Fig. 8. Briefly, IBV infection potentially increases the expression of TLR 3 and 7, leading to recognition of IBV RNA molecules in chicken macrophages. This TLR 3 and 7 recognition of IBV RNA activates the downstream signalling molecules, such as MAPK and JAK, leading to the production of COX-2 and mRNA expression of iNOS and IL-6. The expressions of COX-2 and iNOS lead to the production of PGE2 and NO. These mediators are associated with an increase in IBV replication in chicken macrophages. When PGE2 binding to relevant receptors is blocked, mRNA expressions of iNOS and COX-2 are reduced along with the reduction of IBV genome loads in chicken macrophages. Inhibition of the COX-2/PGE2 pathway at the level of MAPK and JAK-II also results in a reduction of IBV genome loads in chicken macrophages.

In the HTC chicken macrophage cell line, investigations into the effects of natural phenolic COX-2 inhibitors, specifically quercetin, have revealed suppression of lipopolysaccharide-induced IL-1β expression. This suppression occurs through intricate signalling pathways involving NF-κB, MAPK, and cyclic adenosine monophosphate [48]. The biological activities of selective COX-2 inhibitor SC-236 have been demonstrated in MDV-infected chicken embryonic fibroblast cells, as evidenced by studies of Boodhoo *et al.* [27]. Furthermore, oral administration of an FDA-approved COX-2 inhibitor, meloxicam, during MDV infection has shown inhibitory effects on COX-2 activation. This intervention also successfully rescued T cell proliferation at day 21 post-infection, as indicated in the relevant literature [28]. Moreover, the anticipated activity of pharmacological JNK2 inhibition using SP60025 (20 μM) is evident in the reduction of lipopolysaccharide (LPS)-induced IL-1β expression. Additionally, this inhibition is associated with the induction of host β-defensin nine gene through the MAPK pathway in the HTC chicken macrophage cell line [52]. Another anticipated activity that the pharmacological inhibition of PGE2 receptors by EP2, as it has been reported that chemical antagonists of EP2 and EP4 substantially improved survival against lethal Influenza A virus (IAV) infection, whereas PGE2 administration reversed this phenotype in IAV infection and improved the viability of IAV-infected murine macrophage [56], plus it has ben reported IBV-induced apoptosis in chicken macrophage cell line, therefore, it would be a plausibly accepted anticipation that these inhibitor improve cell viability in IBV-infection by blocking PGE2. These findings collectively demonstrate the anticipated activity of pharmacologic COX-2 inhibitors in chicken macrophages and support the potential immunomodulatory effects of these compounds in avian immune responses.

In conclusion, IBV infection leads to activation of the COX-2/PGE2 as well as pro-inflammatory pathways in chicken macrophages. The upregulation of COX-2 expression and subsequent PGE2 production as well as pro-inflammatory signalling can facilitate IBV replication in chicken macrophages. Inhibition of the COX-2/PGE2 pathway not only leads to a reduction in IBV infection in macrophages but also decreases the expression of pro-inflammatory mediators. Further studies are necessary to elucidate the role of the COX-2/PGE2 pathway in the pathogenesis of IBV infection *in vivo*.

Funding information
This research was funded by Natural Science and Engineering Council of Canada discovery grant (Application number RGPIN-2023–03364). Postdoctoral research studies of M.E.M. are funded by the Ministry of Higher Education and Scientific Research of the Arab Republic of Egypt.

Acknowledgements
We acknowledge Dr Guido van Marle, University of Calgary for kindly provided the secondary antibodies for Western blotting. We also acknowledge the guidance of Simmone D'souza of University of Calgary on performing some of the laboratory assays.

Author contributions
Conceptualization, project administration, funding acquisition, and project supervision M.F.A.-C. M.E.M. performed the experiments, contributed to data analysis and discussions, and wrote the first draft of the manuscript. M.F., I.M.I., A.A., M.S.H.H., H.H-M. H.A.R., S.D. and S.M.N. contributed to some experiments. M.F.A.-C. critically revised and finalized the paper.

Conflicts of interest
The authors declare that there are no conflicts of interest.

Ethical statement
The viral titration using embryonated chicken eggs was conducted in accordance with the guidelines of Health Science Animal Care Committee of the University of Calgary (Protocol number: AC19-0011, approved on 19 March 2019).

References

1. Ignjatovic J, Ashton DF, Reece R, Scott P, Hooper P. Pathogenicity of Australian strains of avian infectious bronchitis virus. *J Comp Pathol* 2002;126:115–123.
2. Cavanagh D. Coronavirus avian infectious bronchitis virus. *Vet Res* 2007;38:281–297.
3. Legnardi M, Tucciarone CM, Franzo G, Cecchinato M. Infectious bronchitis virus evolution, diagnosis and control. *Vet Sci* 2020;7:79.
4. Thor SW, Hilt DA, Kissinger JC, Paterson AH, Jackwood MW. Recombination in avian gamma-coronavirus infectious bronchitis virus. *Viruses* 2011;3:1777–1799.

5. Jackwood MW, Jordan BJ. Molecular evolution of infectious bronchitis virus and the emergence of variant viruses circulating in the United States. *Avian Dis* 2021;65:631–636.
6. Rodrigues CMC, Plotkin SA. Impact of vaccines; health, economic and social perspectives. *Front Microbiol* 2020;11:1526.
7. Bhuiyan MSA, Amin Z, Bakar AMSA, Saallah S, Yusuf NHM, *et al*. Factor influences for diagnosis and vaccination of avian infectious bronchitis virus (Gammacoronavirus) in chickens. *Vet Sci* 2021;8:47.
8. Winterfield RW, Hitchner SB. Etiology of an infectious nephritis-nephrosis syndrome of chickens. *Am J Vet Res* 1962;23:1273–1279.
9. Reddy VRAP, Trus I, Desmarets LMB, Li Y, Theuns S, *et al*. Productive replication of nephropathogenic infectious bronchitis virus in peripheral blood monocytic cells, a strategy for viral dissemination and kidney infection in chickens. *Vet Res* 2016;47:70.
10. Amarasinghe A, Abdul-Cader MS, Nazir S, De Silva Senapathi U, van der Meer F, *et al*. Infectious bronchitis corona virus establishes productive infection in avian macrophages interfering with selected antimicrobial functions. *PLoS One* 2017;12:e0181801.
11. Nikitina E, Larionova I, Choinzonov E, Kzhyshkowska J. Monocytes and macrophages as viral targets and reservoirs. *Int J Mol Sci* 2018;19:2821.
12. Murray PJ, Wynn TA. Protective and pathogenic functions of macrophage subsets. *Nat Rev Immunol* 2011;11:723–737.
13. Hirayama D, Iida T, Nakase H. The phagocytic function of macrophage-enforcing innate immunity and tissue homeostasis. *Int J Mol Sci* 2017;19:92.
14. Rasheed A, Rayner KJ. Macrophage responses to environmental stimuli during homeostasis and disease. *Endocr Rev* 2021;42:407–435.
15. Diamond MS, Kanneganti TD. Innate immunity: the first line of defense against SARS-CoV-2. *Nat Immunol* 2022;23:165–176.
16. Chandrasekharan NV, Simmons DL. The cyclooxygenases. *Genome Biol* 2004;5:241.
17. Zarghi A, Arfaei S. Selective COX-2 inhibitors: a review of their structure-activity relationships. *Iran J Pharm Res* 2011;10:655–683.
18. Brock TG, McNish RW, Peters-Golden M. Arachidonic acid is preferentially metabolized by cyclooxygenase-2 to prostacyclin and prostaglandin E2. *J Biol Chem* 1999;274:11660–11666.
19. Kaltschmidt B, Linker RA, Deng J, Kaltschmidt C. Cyclooxygenase-2 is a neuronal target gene of NF-kappaB. *BMC Mol Biol* 2002;3:16.
20. Vane JR, Bakhle YS, Botting RM. Cyclooxygenases 1 and 2. *Annu Rev Pharmacol Toxicol* 1998;38:97–120.
21. Sander WJ, O'Neill HG, Pohl CH. Prostaglandin E2 as a modulator of viral infections. *Front Physiol* 2017;8:89.
22. Kulesza A, Paczek L, Burdzinska A. The role of COX-2 and PGE2 in the regulation of immunomodulation and other functions of mesenchymal stromal cells. *Biomedicines* 2023;11:445.
23. Steer SA, Corbett JA. The role and regulation of COX-2 during viral infection. *Viral Immunol* 2003;16:447–460.
24. Scanes CG. Avian physiology: are birds simply feathered mammals? *Front Physiol* 2020;11:542466.
25. Kwok AHY, Wang Y, Wang CY, Leung FC. Molecular cloning and characterization of chicken prostaglandin E receptor subtypes 2 and 4 (EP2 and EP4). *Gen Comp Endocrinol* 2008;157:99–106.
26. Kwok AHY, Wang Y, Leung FC. Molecular characterization of prostaglandin F receptor (FP) and E receptor subtype 3 (EP3) in chickens. *Gen Comp Endocrinol* 2012;179:88–98.
27. Boodhoo N, Kamble N, Kaufer BB, Behboudi S. Replication of Marek's disease virus is dependent on synthesis of *de novo* fatty acid and prostaglandin E2. *J Virol* 2019;93:e00352–19.
28. Kamble N, Gurung A, Kaufer BB, Pathan AA, Behboudi S. Marek's disease virus modulates T cell proliferation *via* activation of cyclooxygenase 2-dependent prostaglandin E2. *Front Immunol* 2021;12:801781.
29. Najimudeen SM, Abd-Elsalam RM, Ranaweera HA, Isham IM, Hassan MSH, *et al*. Replication of infectious bronchitis virus (IBV) Delmarva (DMV)/1639 variant in primary and secondary lymphoid organs leads to immunosuppression in chickens [published online ahead of print, 2023 Jul 28]. *Virology* 2023;587:109852.
30. Elhamouly M, Terada T, Nii T, Isobe N, Yoshimura Y. Innate antiviral immune response against infectious bronchitis virus and involvement of prostaglandin E2 in the uterine mucosa of laying hens. *Theriogenology* 2018;110:122–129.
31. Chen S, Cheng A, Wang M. Innate sensing of viruses by pattern recognition receptors in birds. *Vet Res* 2013;44:82.
32. Kameka AM, Haddadi S, Kim DS, Cork SC, Abdul-Careem MF. Induction of innate immune response following infectious bronchitis corona virus infection in the respiratory tract of chickens. *Virology* 2014;450–451:114–121.
33. Abdul-Cader MS, Amarasinghe A, Abdul-Careem MF. Activation of toll-like receptor signaling pathways leading to nitric oxide-mediated antiviral responses. *Arch Virol* 2016;161:2075–2086.
34. Lester SN, Li K. Toll-like receptors in antiviral innate immunity. *J Mol Biol* 2014;426:1246–1264.
35. Garren MR, Ashcraft M, Qian Y, Douglass M, Brisbois EJ, *et al*. Nitric oxide and viral infection: Recent developments in antiviral therapies and platforms. *Appl Mater Today* 2021;22:100887.
36. Asif M, Lowenthal JW, Ford ME, Schat KA, Kimpton WG, *et al*. Interleukin-6 expression after infectious bronchitis virus infection in chickens. *Viral Immunol* 2007;20:479–486.
37. Saura M, Zaragoza C, McMillan A, Quick RA, Hohenadl C, *et al*. An antiviral mechanism of nitric oxide: inhibition of a viral protease. *Immunity* 1999;10:21–28.
38. Okino CH, Mores MAZ, Trevisol IM, Coldebella A, Montassier HJ, *et al*. Early immune responses and development of pathogenesis of avian infectious bronchitis viruses with different virulence profiles. *PLoS One* 2017;12:e0172275.
39. Sodano F, Gazzano E, Fruttero R, Lazzarato L. NO in viral infections: role and development of antiviral therapies. *Molecules* 2022;27:2337.
40. Velazquez-Salinas L, Verdugo-Rodriguez A, Rodriguez LL, Borca MV. The role of interleukin 6 during viral infections. *Front Microbiol* 2019;10:1057.
41. Sun X, Wang Z, Shao C, Yu J, Liu H, *et al*. Analysis of chicken macrophage functions and gene expressions following infectious bronchitis virus M41 infection. *Vet Res* 2021;52:14.
42. Hassan MSH, Ojkic D, Coffin CS, Cork SC, van der Meer F, *et al*. Delmarva (DMV/1639) Infectious Bronchitis Virus (IBV) variants isolated in Eastern Canada Show evidence of recombination. *Viruses* 2019;11:1054.
43. Najimudeen SM, Hassan MSH, Goldsmith D, Ojkic D, Cork SC, *et al*. Molecular characterization of 4/91 Infectious Bronchitis Virus leading to studies of pathogenesis and host responses in laying hens. *Pathogens* 2021;10:624.
44. Qureshi MA, Miller L, Lillehoj HS, Ficken MD. Establishment and characterization of a chicken mononuclear cell line. *Vet Immunol Immunopathol* 1990;26:237–250.
45. Mahmoud ME, Ui F, Salman D, Nishimura M, Nishikawa Y. Mechanisms of interferon-beta-induced inhibition of toxoplasma gondii growth in murine macrophages and embryonic fibroblasts: role of immunity-related GTPase M1. *Cell Microbiol* 2015;17:1069–1083.
46. Amarasinghe A, Abdul-Cader MS, Almatrouk Z, van der Meer F, Cork SC, *et al*. Induction of innate host responses characterized by production of interleukin (IL)-1$\beta$ and recruitment of macrophages to the respiratory tract of chickens following infection with infectious bronchitis virus (IBV). *Vet Microbiol* 2018;215:1–10.
47. Han X, Tian Y, Guan R, Gao W, Yang X, *et al*. Infectious bronchitis virus infection induces apoptosis during replication in chicken macrophage HD11 cells. *Viruses* 2017;9:198.

48. Brune K, Patrignani P. New insights into the use of currently available non-steroidal anti-inflammatory drugs. *J Pain Res* 2015;8:105–118.
49. Kim J, Wu D, Hwang DJ, Miller DD, Dalton JT. The para substituent of S-3-(phenoxy)-2-hydroxy-2-methyl-N-(4-nitro-3-trifluoromethyl-phenyl)-propionamides is a major structural determinant of in vivo disposition and activity of selective androgen receptor modulators. *J Pharmacol Exp Ther* 2005;315:230–239.
50. Escobar-Zarate D, Liu YP, Suksanpaisan L, Russell SJ, Peng KW. Overcoming cancer cell resistance to VSV oncolysis with JAK1/2 inhibitors. *Cancer Gene Ther* 2013;20:582–589.
51. Castaño E, Bartrons R, Gil J. Inhibition of cyclooxygenase-2 decreases DNA synthesis induced by platelet-derived growth factor in Swiss 3T3 fibroblasts. *J Pharmacol Exp Ther* 2000;293:509–513.
52. Yang Q, Burkardt AC, Sunkara LT, Xiao K, Zhang G. Natural cyclooxygenase-2 inhibitors synergize with butyrate to augment chicken host defense peptide gene expression. *Front Immunol* 2022;13:819222.
53. Levy G, Guglielmelli P, Langmuir P, Constantinescu SN. JAK inhibitors and COVID-19 [published correction appears in J Immunother cancer. 2023 Apr;11(4)]. *J Immunother Cancer* 2022;10:e002838.
54. Jain NK, Tailang M, Jain HK, Chandrasekaran B, Sahoo BM, *et al*. Therapeutic implications of current Janus kinase inhibitors as anti-COVID agents: a review. *Front Pharmacol* 2023;14:1135145.
55. Alfajaro MM, Choi J-S, Kim D-S, Seo J-Y, Kim J-Y, *et al*. Activation of COX-2/PGE2 promotes sapovirus replication via the inhibition of nitric oxide production. *J Virol* 2017;91:e01656-16.
56. Coulombe F, Jaworska J, Verway M, Tzelepis F, Massoud A, *et al*. Targeted prostaglandin E2 inhibition enhances antiviral immunity through induction of type I interferon and apoptosis in macrophages. *Immunity* 2014;40:554–568.